

433. New linear piezoelectric actuator based on traveling wave

D. Mažeika¹, P. Vasiljev², G. Kulvietis³, S. Vaičiulienė⁴

^{1,3} Vilnius Gediminas Technical University, Saulėtekio al. 11, Vilnius, LT-10223, Lithuania

² Vilnius Pedagogical University, Studentų 39, Vilnius, LT-08106, Lithuania

⁴ Kaunas College, Pramonės pr. 20, LT - 3041 Kaunas, Lithuania

e-mail: ¹dalius.mazeika@fm.vgtu.lt, ²vasiljev@vpu.lt, ³genadijus.kulvietis@fm.vgtu.lt,

⁴vaičiuliene@kauko.lt

(Received 10 January 2009; accepted 10 March 2009)

Abstract. A novel design of linear type piezoelectric actuator is proposed and analyzed in the paper. Actuator has a beam shape with cut-out hole. Traveling wave is generated on the top area of the actuator applying harmonic oscillations on the ends of the beam. These oscillations are generated by two piezoceramic elements and transferred to the ends of the beam. Electrodes of piezoceramic elements are excited by harmonic voltage with phase difference of $\pi/2$. Numerical modeling based on finite element method was performed to find resonant frequencies and modal shapes of the actuator and to calculate the trajectories of contact point movements under different excitation schemes. A prototype of the piezoelectric actuator was built and measurements of top surface oscillations were performed. Results of numerical and experimental studies are discussed.

Keywords: piezoelectric linear actuator, traveling wave, finite element modeling, experimental study.

1. Introduction

Demand of new displacement transducers that can achieve high resolution and accuracy of the driving object increases in nowadays. Piezoelectric actuators have advanced features compare to others and are widely used for different commercial applications [1, 2]. A lot of design and operating principles are investigated to transform mechanical vibrations of piezoceramic elements into elliptical movement of the contact zone of actuator [3, 4, 5]. However summarizing its all the following types of piezoelectric actuators can specified - traveling wave, standing wave, hybrid transducer, and multi-vibration mode [3, 6]. Traveling wave piezoelectric actuators fall under two types – rotary and linear. Rotary type actuators are one of the most popular because of high torque density at low speed, high holding torque, quick response and simple construction. Linear type traveling wave actuators feature these advantages as well but development of these actuators is complex problem [7]. Usually elastic beam is used as the main part of linear traveling wave actuator design and traveling wave oscillations are generated on it [2, 3].

There are two ways of generating a traveling wave in a finite-length beam. The first way is to apply harmonic excitation force at one of the ends of the beam with the task to generate a traveling wave. The other end has to absorb the wave in order to prevent the appearance of standing waves due to the reflection. In order to absorb the incident wave a damper must be

used. (Fig. 1a). The main problem of this method is to find proper dynamic stiffness value of the damper and the beam. The second way consists of using piezoelectric elements placed at specific locations on the beam in order to excite bending vibration mode with a particular phase difference between adjacent exciters - usually it is $\pi/2$ (Fig. 1b). Superposition of these vibrations provides a traveling wave. This method allows changing the traveling wave direction by changing phase of the voltage by π . This way has the problem with boundary conditions. Dynamic stiffness of the beam and clamp must be equal in order to limit reflection of the wave.

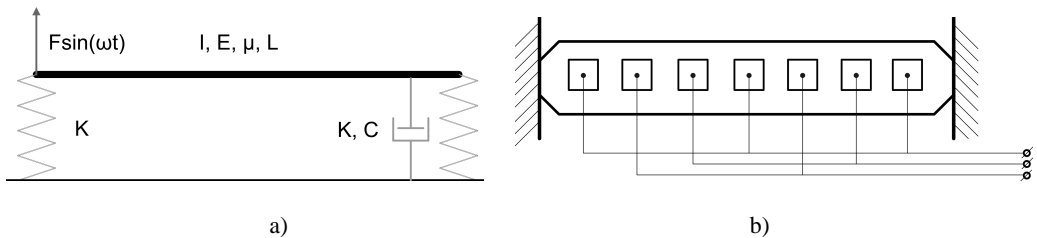


Fig. 1. Principle schemes used to generate traveling wave in the beams: a) traveling wave is generated when on end is excited while another is damped; b) traveling wave is generated when particular zones of the beam is excited

A new idea how to develop linear traveling wave actuator deploying first aforementioned way is described in the paper. Prototype actuator has been made. Numerical modeling of the piezoelectric actuator was carried out using ANSYS software. Experimental study was made and results were analyzed and discussed.

2. Design and Operating Principle of Piezoelectric Actuator

Configuration of actuator includes following parts: a beam shape oscillator with cut-out hole and two rectangular piezoceramic elements that are glued at the bottom of the oscillator (Fig. 2a). Polarization of piezoceramic is oriented along thickness of the elements and piezoelectric effect d_{31} is used for the actuation. There is special contact surface at the middle of top area of the actuator (Fig. 2a). It is used for slider linear driving. Slider can be driven without this contact surface due to the traveling wave generated at the top area of the actuator. Dimensions of the actuator were chosen so that cut-out hole divides actuator into upside and downside beams with thickness ratio $1/2$ (Fig. 2a). Length of the actuator is equal to half of the longitudinal wave. Superposition of flexural and longitudinal modes of the beam is employed to achieve traveling wave type vibrations. Sinusoidal voltage with the different phase by $\pi/2$ is applied on each piezoceramic element.

Operating principle of the actuator is based on the modified first way described in Section 1 of this paper. Traveling wave is generated in the upside beam when mechanical harmonic forces from piezoceramic plates are applied and actuator starts to vibrate. Excitation frequency near 4th flexural mode of upside beam is used. Due to height difference between up and down sides, the downside beam oscillates on 2nd flexural mode at the same frequency (Fig. 2b). Phase difference between oscillations of the ends of upside and downside beams appears when excitation frequency is closed to resonance. Therefore one end of the upside beam is excited while another is damped and travelling wave oscillations without reflection is obtained. Traveling wave motion is illustrated at four points in time during the vibration period of the actuator (Fig. 9).

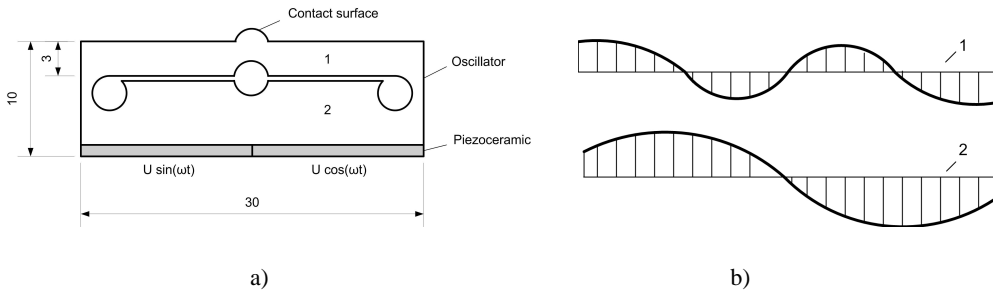


Fig. 2. a) Principle scheme of the actuator; b) diagrams of vibration amplitudes the upside (1) and downside (2) beams of the actuator

3. FEM Modeling of the Actuator

Finite element method was used to perform modal frequency and harmonic response analysis and to calculate trajectories of the driven tips movements. Basic dynamic equation of the piezoelectric actuator are derived from the principle of minimum potential energy by means of variational functionals and for piezoelectric actuator can be written as follows [8, 9, 10]:

$$\begin{cases} [M] \{\ddot{u}\} + [C] \{\dot{u}\} + [K] \{u\} + [T_1] \{\phi_1\} + [T_2] \{\phi_2\} = \{F\} \\ [T_1]^T \{u\} - [S_{11}] \{\phi_1\} - [S_{12}] \{\phi_2\} = \{Q_1\} \\ [T_2]^T \{u\} - [S_{12}]^T \{\phi_1\} - [S_{22}] \{\phi_2\} = \{0\} \end{cases}, \quad (1)$$

where $[M]$, $[K]$, $[T]$, $[S]$, $[C]$ are matrices of mass, stiffness, electro elasticity, capacity, damping respectively, $\{u\}$, $\{F\}$, $\{Q_1\}$ are vectors of nodes structural displacements, external mechanical forces, and charges coupled on the electrodes, $\{\phi_1\}$, $\{\phi_2\}$ are vectors of nodal potentials of the nodes associated with electrodes and vector of nodal potentials calculated during numerical simulation. Mechanical and electrical boundary conditions can be applied to piezoelectric actuator i. e. mechanical displacement of the fixed surfaces of the actuator are equal to zero and electric charge of piezoelements that are not coupled with electrodes are equal to zero too.

Natural frequencies and modal shapes of the actuator are derived from the modal solution of the piezoelectric system:

$$\det([K^*] - \omega^2 [M]) = \{0\}, \quad (2)$$

where K^* is modified stiffness matrix. In case when $\{Q_1\} = 0$ it can be written as follows:

$$[K^*] = [K] + [T][S^{-1}][T^T]. \quad (3)$$

In the case when $\{\phi_1\} = 0$ modified stiffness matrix is:

$$[K^*] = [K] + [T_2][S_{22}^{-1}][T_2^T]. \quad (4)$$

Harmonic response analysis of piezoelectric actuator is carried out applying sinusoidal voltage with different phase on electrodes of piezoelements. Structural mechanical loads are not used in our case so $\{F\} = \{0\}$. Equivalent mechanical forces obtained because of inverse piezoelectric effect can be calculated as follows:

$$\{F_{eq}\} = ([T_2][S_{22}]^{-1}[S_{12}]^T - [T_1]) \{U\} \sin \omega_k t, \quad (5)$$

where $\{U\}$ is vector of voltage amplitudes, applied on the nodes coupled with electrodes. Results of actuator's structural displacements obtained from harmonic response analysis are used for determining the trajectory of contact point movement. Results for structural displacements of the piezoelectric actuator obtained from harmonic response analysis are used to determine the trajectory of the contact point's movement. Admittance values on nodes of piezoceramic finite elements can be determined as the function of frequency:

$$Y_i = \frac{Q_i}{U_i} \omega e^{j(\psi_i + \frac{\pi}{2})}, \quad (6)$$

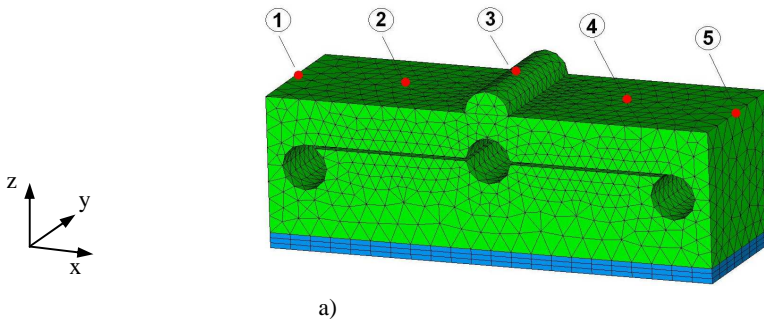
where j refers to the imaginary number, ψ is the phase.

4. Results of Numerical Modeling

Numerical modeling of piezoelectric actuator was performed to validate actuator design and operating principle through the modal and harmonic response analysis. FEM software ANSYS 10.0 was employed for simulation. FEM model (Fig. 3a) was built and following materials were used for actuator modeling: bronze was used for the oscillator and piezoceramic PZT-8 was used for piezoelements.

Modal analysis of piezoelectric actuator was performed to find proper resonance frequency. Material damping was assumed in the finite element model. No structural boundary conditions were applied. Examining results of modal analysis it was determined that vibration mode No. 19 (54.97 kHz) is exploitable for further investigation. Actuator's modal shape compose of 4th flexural modal shape of the upside beam and 2nd flexural mode at downside beam at this frequency (Fig. 3b).

Harmonic response analysis was performed with the aims to find out the actuator's response to sinusoidal voltage applied on electrodes of the piezoceramic elements, to verify operating principle and to calculate trajectories of the arbitrary contact points' movements. The contact points are located at the middle line of the oscillator's top surface (Fig. 3a). Analyzing oscillation characteristics of arbitrary contact points, travelling wave vibrations on the upside beam of the actuator will be manifested. Excitation scheme of the electrodes was used as shown in Fig. 2a. A 60V AC signal was applied. A frequency range from 50 kHz to 60 kHz with a solution at 0.25 kHz intervals was chosen and adequate response curves of arbitrary contact points' No.1 – 5 oscillation amplitudes and phases were calculated. Amplitude – frequency characteristic of longitudinal (Fig. 4a) and flexural (Fig. 4b) oscillations of the arbitrary contact points are given as results of calculations.



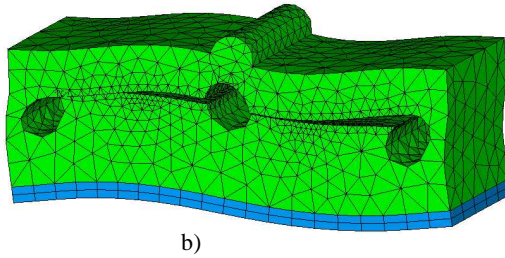
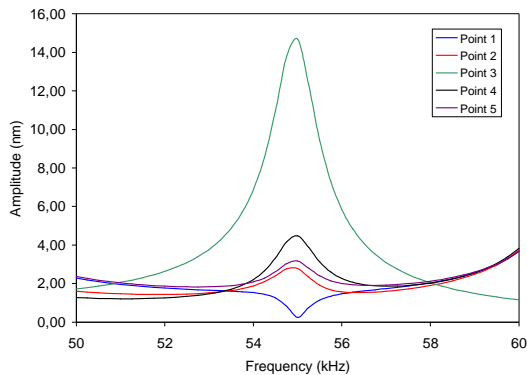
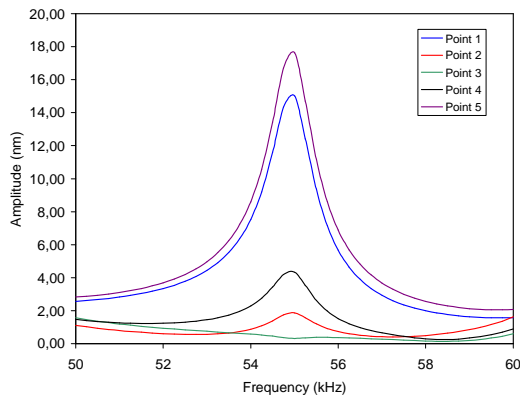


Fig. 3. a) Finite element model of the actuator and location of arbitrary contact points on top surface. b) Vibration mode of the actuator at 54.97 kHz.



a)



b)

Fig. 4. Amplitude-frequency characteristic of arbitrary contact points No.1-5: a) longitudinal and b) flexural oscillations

Graphs of oscillation amplitudes of the arbitrary contact points indicate that resonant oscillations are obtained at 55 kHz. Resonant at the same frequency is illustrated the curve of electrical input admittance over the frequency range 50-60 kHz (Fig. 6). By observing results of harmonic response analysis it can be indicated that graph or the phase differences between flexural and longitudinal oscillations close to 0 or π at resonant frequency and significantly differs from 0 when excitation frequency is lower by 1-3 kHz than resonant (Fig. 5). This

indicates that trajectory of motion of the arbitrary contact points is closed to straight line motion and standing wave oscillations are obtained at the resonant frequency however elliptic trajectory of motion and traveling wave oscillations are generated when frequency is lower then resonant (Fig. 10).

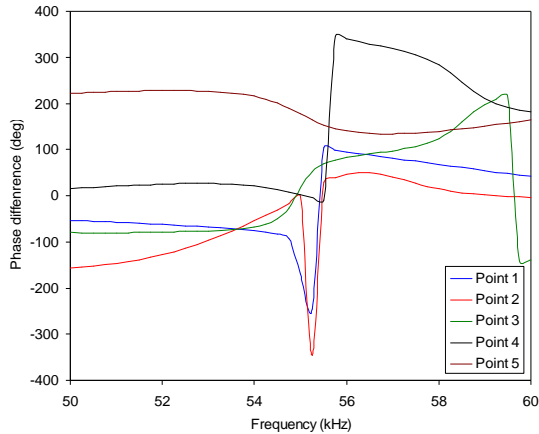


Fig. 5. Diagram of the phase difference between flexural and longitudinal oscillations versus frequency of arbitrary contact points No.1-5

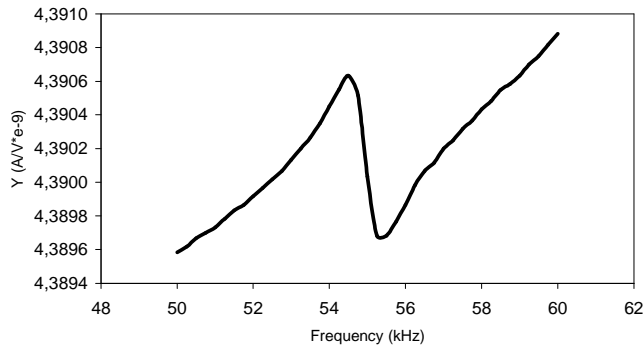


Fig. 6. Electrical input admittance versus frequency

When examining oscillations of the arbitrary point No.1 and No.5 and oscillations of the corresponding ends of the piezoceramic elements (Fig. 7) it can be noticed, that oscillations of the left outside end of piezoceramic element and point No.1 have the phase difference close to $\pi/2$ while phase different between point No.5 and right outside end of piezoceramic element is close to π at frequency 1-3 kHz lower than resonant. This means that left side of the upside beam is excited while right side is damped. Phase difference changes to values closed to 0 at resonant frequency so standing wave oscillation are generated in the system.

Fig. 8 presents positions of actuator's top surface oscillations during half of the vibration period when excitation frequency is set to 53 kHz. Traveling wave type oscillations can be clearly indicated especially at the middle of the actuator length. Traveling wave oscillations of the actuator at the same frequency is illustrated at four points in time during the vibration period in Fig. 9.

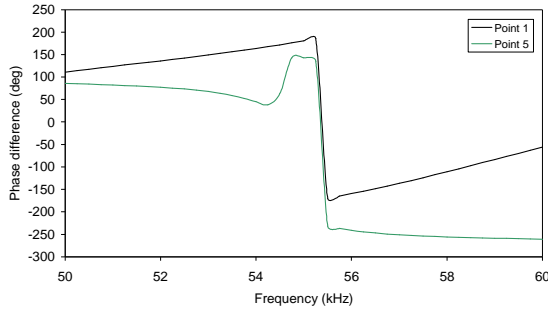


Fig. 7. Diagram of the phase difference between flexural oscillations versus frequency of arbitrary contact points No.1,5 and outside ends of piezoceramic elements

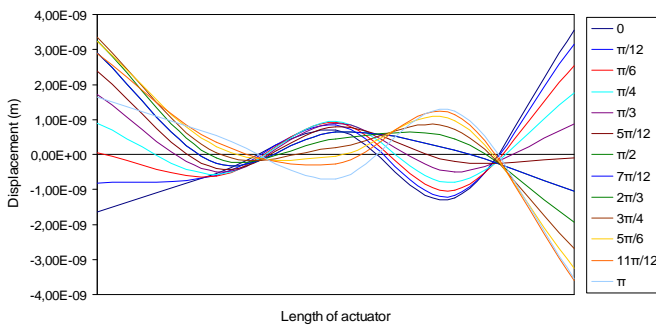


Fig. 8. Top surface oscillations during half of the vibration period. Excitation frequency 53 kHz

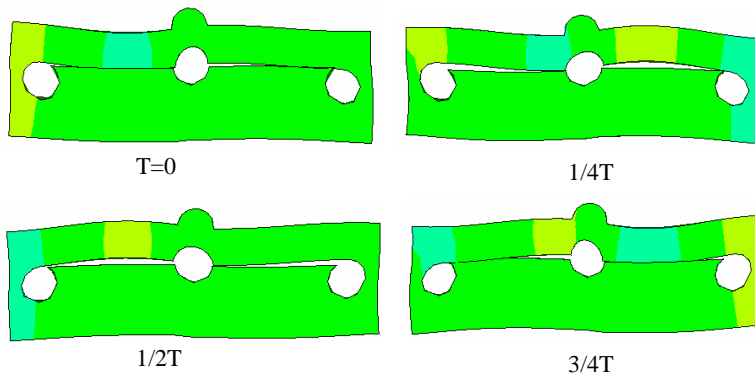


Fig. 9. Position of the actuator during the vibration period. Excitation frequency 53 kHz

Applying results of harmonic response analysis, trajectories of motion of contact points No.1 - 5 were calculated at excitation frequency range 50 – 60 kHz. Fig. 10 illustrates these trajectories at frequencies 54 kHz and 55 kHz respectively. It can be seen that trajectories in both graphs have elliptic shape but ratio of the major and minor axis are different. Compound parameters of the ellipses i. e. dependencies of the ratio of major and minor axis and rotation of major axis are given in Fig. 11.

Analyzing ratio between major and minor axis of the ellipsis it can be indicated that peak of the ratio appears at resonant frequency. It means that trajectories of motion are close to straight

line at resonance and motion close to standing wave type is achieved. Rotation angle of major axis of arbitrary contact points are given in Fig. 11b. It can be indicated that the rotation angle of different points significantly differs at resonant frequency while receding from resonance, rotation angle of all arbitrary points approaches to particular value. Graphs in Fig. 11 can be used to define operating frequency of actuator based on parameters of the ellipses.

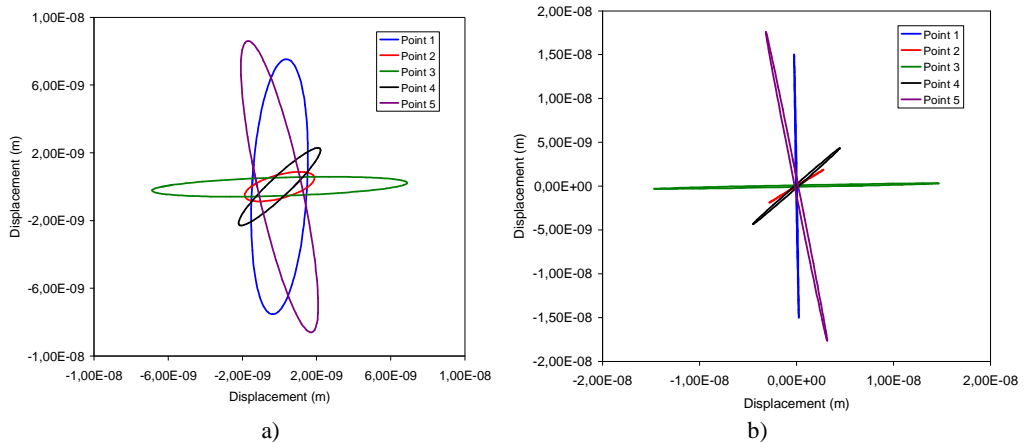


Fig. 10. Trajectories of the points No.1 - 5 movements at excitation frequencies: a) 54 kHz and b) 55 kHz

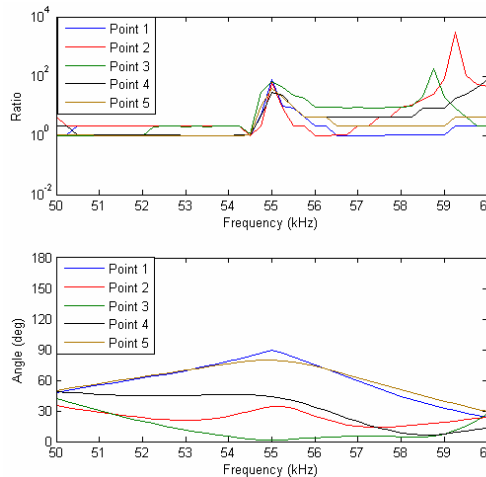


Fig. 11. Trajectories dependencies of the ratio of major and minor axis and rotation of major axis are given

5. Experimental Study

A prototype actuator was made for experimental study (Fig. 12). The aims of experiment were to evaluate operating principle of the actuator and to verify results of the numerical modeling. Impedance-frequency characteristics of the actuator were determined with the help of the 4192A LF Impedance Analyzer (Hewlett Packard). Top surface's oscillations were measured using a vibrometer POLYTEC CLV 3D. The resonant frequency at 56.25 kHz was determined by means of electrical impedance study. The difference between experimental and numerical resonant frequencies is 2.2%.

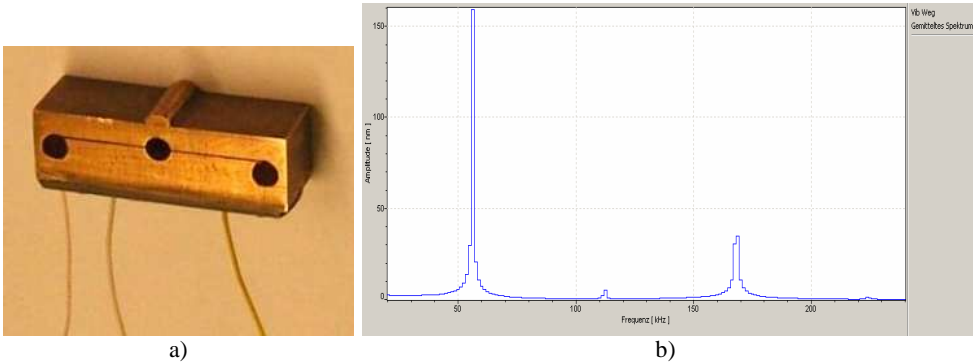


Fig. 12. Experimental results: a) prototype actuator; b) amplitude – frequency characteristics of arbitrary contact point of the actuator

Measurements of the actuator top surface oscillations were done using excitation scheme as shown in Fig. 2a. Results of actuator's top surface vibrations measurements are given in Fig. 13. They confirm results of numerical modelling that travelling wave oscillations is achieving at top surface of the actuator. The difference between the contact points' oscillation amplitudes obtained in numerical modelling and measured in experiments is 10-15%.

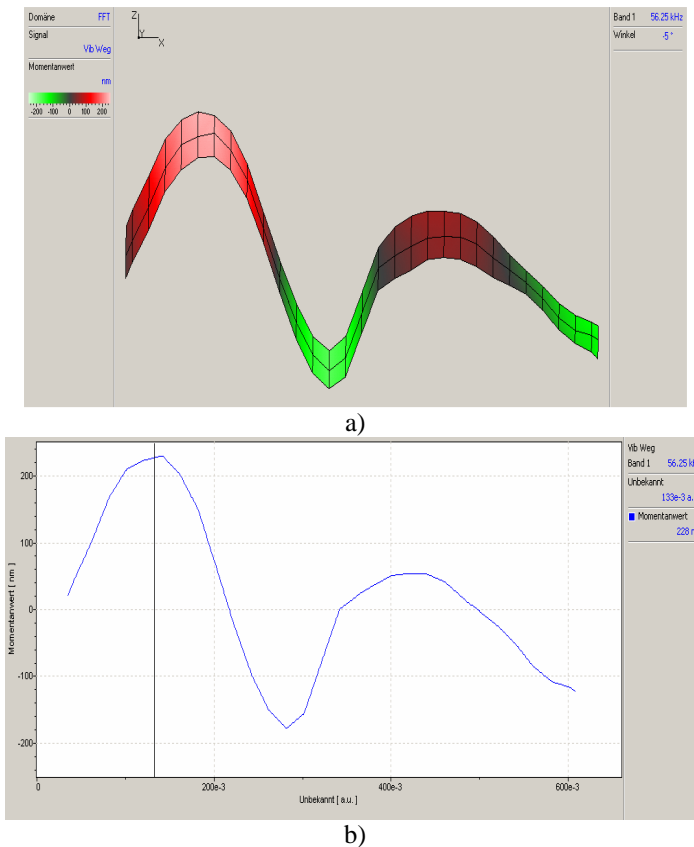


Fig. 13. Distribution of oscillation amplitudes on top surface of the actuator: a) 3D view; b) at the middle line of top surface

Conclusions

A new linear traveling wave type piezoelectric actuator was developed. Numerical and experimental studies confirmed that traveling wave can be generated in the linear type actuator when only two piezoceramic elements are used for excitation. Elliptic trajectories of the five arbitrary points of the top surface of the actuator were calculated and traveling wave oscillations have been shown. Experimental study has confirmed that travelling wave oscillations are obtained on top surface of the actuator. Results of numerical modeling and experimental study are in good agreement.

Acknowledgement

This work has been supported by Lithuanian State Science and Studies Foundation, Project No B-07017, "PiezoAdapt", Contract No K-B16/2008-1.

References

- [1] **Uchino K., Giniewicz J.** Micromechatronics, Marcel Dekker Inc, New York, 2003.
- [2] **Sashida T., Kenjo T.** An Introduction to Ultrasonic Motors. Oxford Press, 1994.
- [3] **Uchino K.** Piezoelectric ultrasonic motors: overview. *Journal of Smart Materials and Structures*, Vol.7, 1998, pp. 273-285.
- [4] **Bansevicius R., Barauskas R., Kulvietis G., Ragulskis K.** Vibromotors for Precision Microrobots. Hemisphere Publishing Corp., USA, 1988.
- [5] **Bansevicius R., Kulvietis G., Mazeika D.** Piezoelectric Wide Range Laser Deflecting/Scanning Devices with one and two Degrees-of-Freedom: State of the Art and Latest Developments. Proceedings of 11th Int. Conference "Actuator 08", 2008. pp. 117-120.
- [6] **Hemsel T., Wallaschek J.** Survey of the present state of the art of piezoelectric linear motors. *Ultrasonics*, Vol. 38, 2000, pp. 37-40
- [7] **Friend J., Nakamura K., Ueha S.** A Traveling-Wave Linear Piezoelectric Actuator with Enclosed Piezoelectric Elements—The "Scream" Actuator. Proceedings of the 2005 IEEE/ASME International Conference on Advanced Intelligent Mechatronics Monterey, California, USA, 2005, pp.183-188.
- [8] **Vasiljev P., Borodinas S., Yoon S.-J., Mazeika D., Kulvietis G.** The actuator for micro moving of a body in a plane. *Materials Chemistry and Physics*, vol. 91, 1(2005), pp. 237-242.
- [9] **Vasiljev P., Mažeika D., Kulvietis G.** Modelling and analysis of omni-directional piezoelectric actuator. *Journal of Sound and Vibration*, Vol. 308, Issue 3-5, Elsevier, 2007, 867-878 pp.
- [10] **Frangi A., Corigliano A., Binci M., Faure P.** Finite Element Modelling of a Rotating Piezoelectric Ultrasonic Motor. *Ultrasonics*, Vol. 43, Is. 9, 2005, pp. 747-755.